

# AdvLoRA: Adversarial Low-Rank Adaptation of Vision-Language Models

Yuheng Ji\*

jyuheng2023@ia.ac.cn  
The State Key Laboratory of  
Multimodal Artificial Intelligence  
Systems, Institute of Automation  
The School of Artificial Intelligence,  
University of Chinese Academy of  
Sciences  
Beijing City, China

Zhao Zhang

Beijing University of Posts and  
Telecommunications  
Beijing City, China

Xingwei Zhang

The State Key Laboratory of  
Multimodal Artificial Intelligence  
Systems, Institute of Automation  
The School of Artificial Intelligence,  
University of Chinese Academy of  
Sciences  
Beijing City, China

Yue Liu\*

Institute of Data Science,  
National University of Singapore  
Singapore

Yuting Zhao

The State Key Laboratory of  
Multimodal Artificial Intelligence  
Systems, Institute of Automation  
The School of Artificial Intelligence,  
University of Chinese Academy of  
Sciences  
Beijing City, China

Xinwang Liu<sup>†</sup>

School of Computer Science and  
Technology, National University of  
Defense Technology  
Changsha City, China

Zhicheng Zhang

The State Key Laboratory of  
Multimodal Artificial Intelligence  
Systems, Institute of Automation  
The School of Artificial Intelligence,  
University of Chinese Academy of  
Sciences  
Beijing City, China

Gang Zhou

Beijing University of Posts and  
Telecommunications  
Beijing City, China

Xiaolong Zheng<sup>†</sup>

The State Key Laboratory of  
Multimodal Artificial Intelligence  
Systems, Institute of Automation  
The School of Artificial Intelligence,  
University of Chinese Academy of  
Sciences  
Beijing City, China

## ABSTRACT

Vision-Language Models (VLMs) are a significant technique for Artificial General Intelligence (AGI). With the fast growth of AGI, the security problem become one of the most important challenges for VLMs. In this paper, through extensive experiments, we demonstrate the vulnerability of the conventional adaptation methods for VLMs, which may bring significant security risks. In addition, as the size of the VLMs increases, performing conventional adversarial adaptation techniques on VLMs results in high computational costs. To solve these problems, we propose a parameter-efficient Adversarial adaptation method named AdvLoRA by Low-Rank Adaptation. At first, we investigate and reveal the intrinsic low-rank property during the adversarial adaptation for VLMs. Different from LoRA, we improve the efficiency and robustness of adversarial adaptation by designing a novel reparameterizing method based on parameter clustering and parameter alignment. In addition, an adaptive parameter update strategy is proposed to further improve the robustness. By these settings, our proposed AdvLoRA alleviates the model security and high resource waste problems. Extensive experiments demonstrate the effectiveness and efficiency of the AdvLoRA.

\* Both authors contributed equally to this research.

<sup>†</sup> Corresponding Author

## CCS CONCEPTS

• **Computing methodologies** → **Artificial intelligence**.

## KEYWORDS

Adversarial robustness, Low-Rank adaptation, Vision-Language models

## 1 INTRODUCTION

Artificial General Intelligence (AGI), which aims to create intelligent agents that can perform as well as or better than humans on a wide range of cognitive tasks, is a promising topic for both research and industrial products [27, 76]. As vision and language are the most important information of intelligence, Vision-Language Models (VLMs) have become a significant technique for achieving AGI [1, 20].

In recent years, the adaptation of VLMs aims to improve the performance on different downstream tasks and has become a hot research topic. However, through extensive experiments, we find the vulnerability of the conventional adaptation methods, e.g., Full Fine-Tuning (FFT) [99, 103, 109], Linear Probe (LP), LoRA [33], Unidapter [119], and Aurora [121] for VLMs, which may bring

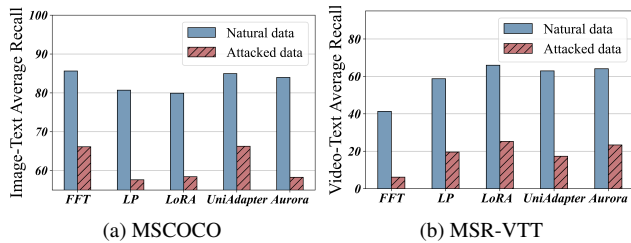


**Figure 1: The vulnerability of vision-language model adaptation methods on natural data and attacked data of two datasets.**

significant security threats in various domains, such as facial recognition [91, 94], medical analysis [22, 66] and autonomous driving [21, 111]. As shown in Figure 1, we conduct adaptation experiments of VLMs on the natural and attacked data of the MSCOCO [118] and MSR-VTT [122] datasets. From these experimental results, we find that the average performance drops about 30.98% on the attacked data. To solve this problem, various techniques are proposed against adversarial attacks by data augmentation [73, 95], attack detection [50, 70] and adversarial training [28, 52]. As the most effective defense strategy, adversarial training enhances the adversarial robustness of VLMs by retraining the model on mined adversarial examples [67, 75, 92].

However, as the sizes of VLMs increase, the conventional adversarial training method with full parameter updating to improve the adversarial robustness of VLMs will lead to high computing and storage costs. In recent years, Parameter-Efficient Fine-Tuning (PEFT) technology has garnered widespread attention as a novel adaptation paradigm due to its significant success in adapting large-scale pre-trained models. PEFT technologies can adapt VLMs with extremely small additional tunable parameters and achieve comparable or better performance than FFT methods. While PEFT technologies have demonstrated remarkable success in natural scenarios, their application in adversarial attack scenarios remains largely uncharted territory. But simply applying the adversarial training on the conventional adaptation methods will lead to 1) limited defense performance and 2) high computational and storage costs. To verify our points, we visualize the adversarial robustness performance and the tunable parameter number of different adversarial adaptation methods in Figure 2. From the results, we find that the existing adaptation methods such as FFT and UniAdapter will lead to large parameter costs. Besides, LoRA, LP, and Aurora are not robust to adversarial attacks.

To solve these problems, we aim to develop a parameter-efficient adversarial adaptation method termed AdvLoRA to effectively and efficiently improve the robustness of VLMs against attacks. At first, similar to LoRA, the intrinsic low-rank property of adversarial adaptation for VLMs is revealed. Secondly, we improve LoRA with a novel reparameterizing technology. Concretely, we regard the rank of LoRA as the number of cluster centers and utilize the clustering algorithm to reparameterize LoRA from the weight matrices of VLMs. The weight matrices are decoupled into the clustering centers and the clustering distribution matrices. Subsequently, we impose constraints on their product to align with the parameter distribution

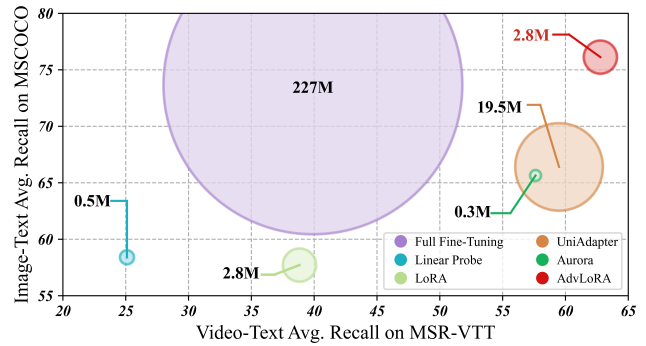


**Figure 2: Adversarial robustness and tunable parameter number of adversarial adaptation methods on two dataset.**

of the original weight matrix. Moreover, we design an adaptive parameter update strategy to improve the robustness further. Through these settings, we effectively and efficiently facilitate the adversarial adaptation of VLMs. The contributions of this paper are summarized as follows.

- We demonstrate the vulnerability of VLMs with different adaptation methods to adversarial attacks via experiments.
- We investigate and reveal the intrinsic low-rank property during the adversarial adaptation for vision-language models.
- We propose a novel parameter-efficient adversarial adaptation method named AdvLoRA with parameter clustering, parameter alignment, and adaptive parameter update.
- We are the first to introduce the adversarial adaptation for vision-language models. Extensive experiments demonstrate the effectiveness and efficiency of our proposed method.

## 2 RELATED WORK

### 2.1 Vision-Language Models

Vision-Language Models (VLMs) have demonstrated success in addressing diverse vision-language downstream tasks, including cross-modal retrieval[25, 34, 108] and cross-modal generation[9, 83, 84, 88]. Leveraging large-scale multi-modal data and self-supervised training, VLMs learn semantic associations across modalities and establish a generalized multi-modal representation subspace, so that it can be regarded as fundamental models to address cross-modal tasks. The architecture of VLMs typically consists of three parts, the text encoder, the image encoder, and the multi-modal fusion module. The text encoder encodes textual data, typically utilizing structures such as word embeddings[38, 71], BERT[17, 64], and GPT[81, 82]. The image encoder, on the other hand, encodes visual data, commonly employing structures like CNN[35, 39], Fast R-CNN[14, 26, 64], and ViT[38, 41, 42]. The multi-modal fusion module is typically based on the transformer architecture[93] and can be categorized into three forms: encoder-based[42, 64, 81], decoder-based[84], and encoder-decoder-based[100]. Benefiting from the advantages of both the encoder and decoder architecture, encoder-decoder-based VLMs can achieve better performance on both cross-modal understanding and generating tasks, like BLIP[41]. In this paper, we explore the adversarial robustness of BLIP. Recently, with the success of Large

Language Models (LLMs), researchers have embarked on the exploration of how to enhance VLMs’ comprehension of multimodal data through the integration of LLMs. Examples include BLIP-2 [40], Flamingo [4], LLaVA [48, 49], Qwen-VL [8], and others.

## 2.2 Parameter-efficient Tuning on VLMs

Parameter-efficient Tuning technologies are first proposed to alleviate the heavy training and storage cost in the process of adaptation of pre-trained models. Adaptation is an effective way to help pre-trained models solve the downstream tasks, which usually occurs when pre-trained models perform a specific task that task-related data distribution is different from training data. However, as the size of VLMs increases, traditional adaptation technologies such as FFT are inefficient and costly [99, 103, 109]. Recently, inspired by methods from natural language processing [16, 32, 33, 45, 53, 110] and computer vision [7, 37, 85] domains, some approaches designed for VLM are proposed, which aim to adapt frozen VLMs to downstream tasks by introducing extremely small learnable parameters. Although it has fewer learnable parameters, its effect can equal or even exceed that of the full-parameters tuning. These can be roughly divided into three types: adapter-based [24, 119], prompt-based [65, 105, 115], and LoRA-based [3, 15, 18, 31, 61, 69, 74, 80, 98, 112, 114]. LoRA-based approaches have received considerable attention due to their fewer learnable parameters, no additional input, and no additional inference latency. In this paper, we explore the LoRA-based approach to VLMs from the clustering perspective.

## 2.3 Adversarial Robustness on VLMs

Some researchers have proven that artificial neural networks including VLMs are vulnerable to human-unrecognized attacks [10, 44, 113]. Specifically, adding additional perturbations to input can cause VLMs to make the incorrect decision with high confidence. To improve adversarial robustness on VLMs, most works focus on data augmentation [10, 102] and adversarial training [23, 68]. Considered one of the most effective methods, adversarial training can improve the adversarial robustness of VLMs by injecting adversarial inputs into the training procedure through a min-max formulation [23, 68]. However, adopting adversarial training to VLMs is costly due to the huge parameters that need to be updated. To our best knowledge, TeCoA [68] is so far the only adversarial training method using parameter-efficient tuning technology to improve the adversarial robustness of VLMs. However, TeCoA focuses on single-modality downstream tasks (image classification) and has not been studied in the cross-modal tasks. In this paper, we explore the adversarial training to LoRA-based approach and try to improve the adversarial robustness of cross-modal tasks with VLMs inexpensively.

## 2.4 Clustering Algorithm

Clustering is a fundamental yet challenging task that aims to group the samples into separated clusters in an unsupervised manner. Benefit from the ability to mine unlabeled data. At the early stage, various traditional clustering methods [19, 30, 86, 87, 96] are proposed. For example, the classical  $k$ -Means clustering [30] group samples via iteratively updating the cluster centers and cluster assignment. In recent years, inspired by the stunning performance of deep learning, deep clustering [6, 43, 46, 72, 79, 89] has become a fast-growing

research spot. For example, Xie et. al. propose DEC [104] to perform clustering via deep learning. Concretely, they first initialize the cluster centers via  $k$ -Means clustering on samples and then optimize clustering distribution with a Kullback–Leibler divergence clustering loss [104]. Additionally, IDEC [29] is proposed to improve DEC by reconstructing original information from latent embeddings. Besides, JULE [107] is proposed to perform clustering via iteratively learning data embeddings and clustering assignments. Similarly, DeepCluster [11] also updates the deep network according to the clustering assignments in turn. In addition, an online method named SwAV [12] clusters the data and keeps the consistency between cluster assignments produced from different views of the same image. In DINO [13], a momentum encoder is adopted to alleviate representation collapse. Furthermore, Qian proposes SeCu [78] by designing a stable cluster discrimination task and a new hardness-aware clustering criterion. In addition to image data, deep clustering is also widely applied to graphs [54–59], texts [2, 36, 51, 90], and recommendation [60]. However, parameter clustering is relatively rare. It is worth taking advantage of the unsupervised learning ability of clustering to separate the parameters into different clusters.

## 3 METHOD

In Section 3.1, we first define the cross-modal retrieval. Subsequently, addressing the vulnerability of VLMs to adversarial attacks, we introduce an adversarial training module in Section 3.2 to enhance the model’s adversarial robustness. Finally, to mitigate the high cost associated with adversarial training, we present an adaptation module in Section 3.3, which maintains the VLMs’ adversarial robustness while reducing the expenses of adversarial training.

### 3.1 Task Definition

**3.1.1 Cross-Modal Retrieval.** Cross-modal retrieval aims to utilize information from one modality to retrieve semantically relevant information from another. We select cross-modal retrieval as our benchmark task due to its efficacy in assessing the quality of cross-modal representation learning in VLMs. Under adversarial attacks, cross-modal retrieval serves as an effective metric for evaluating whether models can learn robust feature representations.

Taking image-to-text retrieval as an example, given an image  $v_i$ , its semantic representation  $\mathbf{z}_i^v = \mathcal{F}_v(v_i)$  is used to compute the cosine similarity with each textual representation  $\mathbf{z}_j^w$  within the text database as follows.

$$\text{sim}(\mathbf{z}_i^v, \mathbf{z}_j^w) = \frac{\mathbf{z}_i^v \cdot \mathbf{z}_j^w}{\|\mathbf{z}_i^v\| \|\mathbf{z}_j^w\|}, \quad (1)$$

where  $\mathbf{z}_j^w = \mathcal{F}_w(w_j)$  represents the semantic representation derived from the textual data  $w_j$  after feature extraction via the text encoder  $\mathcal{F}_w$ . Then we select the highest similarity text data as the retrieval results. Under adversarial attacked, robust VLMs could learn semantically invariant feature representations so that they will not be misled by small perturbations.

### 3.2 Adversarial Training Module

Extensive experimentation demonstrated that both VLMs and their variants adapted with PEFT methods are susceptible to adversarial attacks, as illustrated in Figure 1 and the Appendix. Consequently,

in this subsection, we design an adversarial training module to enhance the adversarial robustness of VLMs. We begin by introducing the concept of adversarial attacks, followed by the presentation of adversarial training as an effective defense technology for enhancing adversarial robustness.

**3.2.1 Adversarial Attack.** Adversarial attacks  $\delta$  is a tensor added to the natural image  $v$ ,  $v_a = v + \delta$ , aiming to fool the model into making the incorrect decision as formulated.

$$v_a = \arg \max_{v_a} \mathcal{L}(v_a, w), \quad \text{s.t.} \quad \|v_a - v\|_p \leq \varepsilon, \quad (2)$$

where  $p$  donates the  $p$ -norm, and  $\varepsilon$  donates the restriction value of values, which is often set to be smaller than  $8/255$ . Thus, the adversarial attacks are imperceptible to humans. In this paper, we focus on adversarial attacks on visual data, as attacks on natural language are readily perceptible to humans. Therefore, it is practically significant and more challenging to make attacks on visual data. Concretely, we utilize PGD [67] to generate  $v_a$  as follows.

$$v_a = \prod \left\{ \text{clip}_\varepsilon(v + \xi \cdot \text{sign}(\nabla_v \mathcal{L}(v, w))) \right\}, \quad (3)$$

where  $\text{sign}(\nabla_v \mathcal{L}(v, w))$  denotes the sign value of the back-propagated gradient. Besides,  $\xi$  is the step size of each iteration. And  $\text{clip}_\varepsilon(x) = \min(x, \varepsilon)$  clips each value of  $x$  to be smaller than  $\varepsilon$  and return  $\varepsilon$  when the value of any dimension exceeds  $\varepsilon$ .  $\prod\{\cdot\}$  denotes the iterative procedure. In this manner,  $v_a$  can fool the model to make the incorrect decision. Notably, for video data, we treat it as a collection of images and attack 20% of the frames by randomly sparse sampling [101].

**3.2.2 Adversarial Training.** Adversarial training technologies refer to retraining the model on attacked data, which can learn semantically invariant features under adversarial attacks. Adversarial training aims to minimize the following objective.

$$\theta = \arg \min_{\theta} \mathcal{L}(v_a, w), \quad (4)$$

where  $\theta$  donates the parameters of the model.

### 3.3 Adaptation Module

Although adversarial training can effectively enhance VLMs' adversarial robustness, it requires updating all parameters based on gradient information, leading to a significant cost overhead. To alleviate this issue, in this subsection, we propose an adaptation module that performs adversarial training on LoRA to reduce the number of learnable parameters, achieving parameter-efficient adversarial adaptation. We first provide a brief introduction to LoRA, followed by the introduction of clustering reparameterization and parameter alignment methods, as well as an adaptive parameter update strategy, to facilitate adversarial adaptation.

**3.3.1 LoRA.** LoRA achieves parameter-efficient adaptation by updating two low-rank matrices attached to the frozen pre-trained weights. Specifically, given the pre-trained weights  $\mathbf{W}_0 \in \mathbb{R}^{m \times n}$ , and the LoRA matrices  $\mathbf{A} \in \mathbb{R}^{m \times k}$ ,  $\mathbf{B} \in \mathbb{R}^{k \times n}$ , the input  $\mathbf{X}^{(l-1)} \in \mathbb{R}^{b \times m}$  is processed through the following computation to obtain the output  $\mathbf{X}^{(l)} \in \mathbb{R}^{b \times n}$  as follows.

$$\mathbf{X}^{(l)} = \mathbf{X}^{(l-1)} \mathbf{W}_0 + \mathbf{X}^{(l-1)} \mathbf{A} \mathbf{B}, \quad (5)$$

where  $k \ll \min(m, n)$ . And  $\mathbf{A}$  and  $\mathbf{B}$  are initialized as follows.

$$\mathbf{A} \sim \mathcal{N}(0, \sigma^2), \quad \mathbf{B} = \mathbf{0}, \quad (6)$$

where  $\mathcal{N}$  denotes the Gaussian distribution.

During the adaptation process,  $\mathbf{W}_0$  is fixed, while  $\mathbf{A}$  and  $\mathbf{B}$  are updated via the gradient descent methods. In our proposed model, AdvLoRA, we freeze  $\mathbf{W}_0$  and solely update  $\mathbf{A}$ ,  $\mathbf{B}$  through adversarial adaptation to achieve adversarial robustness in the model as follows.

$$\theta_{\mathbf{A}, \mathbf{B}} = \arg \min_{\theta_{\mathbf{A}, \mathbf{B}}} \mathcal{L}(v_a, w). \quad (7)$$

Our model adheres to conventional practice by incorporating LoRA into both the attention modules and feed-forward networks in BLIP.

#### 3.3.2 Reparameterization and Adaptive Parameter Update.

The primary distinction between AdvLoRA and other LoRA-like methods lies in the parameterization process of the matrices  $\mathbf{A}$ ,  $\mathbf{B}$ . In the original LoRA, a random Gaussian initialization for  $\mathbf{A}$  and zero for  $\mathbf{B}$ , so  $\mathbf{A}\mathbf{B}$  is zero at the beginning of adaptation. In contrast, our model, AdvLoRA, initially performs clustering on the weight matrix  $\mathbf{W}_0$  of the pre-trained model, treating the rank  $k$  of LoRA as the number of cluster centers. Specifically, given an weight matrix  $\mathbf{W} \in \mathbb{R}^{m \times n}$  and the rank  $k$ , we first randomly initialize  $k$  cluster center  $\mathbf{C} = \{\mathbf{c}_1, \mathbf{c}_2, \dots, \mathbf{c}_k\}$ . Then, for each column  $\mathbf{w}_i$  of  $\mathbf{W}$ , compute the distances to each cluster center  $\mathbf{c}_j$  and assign  $\mathbf{w}_i$  to the closest cluster as follows.

$$\text{cluster}_i = \arg \min_j \|\mathbf{w}_i - \mathbf{c}_j\|_2. \quad (8)$$

Then update the cluster centers by computing the mean of all data points assigned to each cluster as follows.

$$\mathbf{c}_j = \frac{1}{|S_j|} \sum_{\mathbf{w}_i \in S_j} \mathbf{w}_i, \quad (9)$$

where  $S_j$  is the set of columns of  $\mathbf{W}$  assigned to cluster  $j$ . Repeat the above steps until the cluster centers no longer change significantly or a maximum number of iterations is reached. In this manner, we obtain the cluster center embeddings  $\mathbf{C} \in \mathbb{R}^{k \times n}$  and the distance assignment matrix  $\mathbf{D} \in \mathbb{R}^{m \times k}$ , where each element  $d_{ij}$  represents the distance between the  $\mathbf{w}_i$  and cluster center  $\mathbf{c}_j$ . The distance assignment matrix  $\mathbf{D}$  can be computed using the following formula.

$$\mathbf{d}_{ij} = \|\mathbf{w}_i - \mathbf{c}_j\|_2. \quad (10)$$

And the cluster center representation matrix  $\mathbf{C}$  is simply the matrix of cluster centers as follows.

$$\mathbf{C} = [\mathbf{c}_1, \mathbf{c}_2, \dots, \mathbf{c}_k]. \quad (11)$$

After the parameter clustering, the clustering assignment matrix  $\mathbf{D} \in \mathbb{R}^{m \times k}$  and the parameter center  $\mathbf{C} \in \mathbb{R}^{k \times n}$  can be represented the  $\mathbf{A} \in \mathbb{R}^{m \times k}$  and  $\mathbf{B} \in \mathbb{R}^{k \times n}$  in the original LoRA method. By these settings, we provide a better reparameterization of the tunable parameters in LoRA. It separates the parameters into different clusters, which have different functions in the whole network.

After obtaining the matrices  $\mathbf{A}$  and  $\mathbf{B}$ , we further impose constraints on their product  $\mathbf{A}\mathbf{B}$  to align with the parameter distribution of the original weight matrix  $\mathbf{W}_0$  as follows.

$$\min \|\mathbf{W}_0 - \mathbf{A}\mathbf{B}\|_2. \quad (12)$$

In this manner, we can guarantee the zero initialization of **AB** at the beginning of the training.

During the process of model adversarial adaptation, we design an adaptive update parameter,  $\alpha$ , to facilitate the model’s adaptive learning of robust semantic representations as follows.

$$Y = XW_0 + \alpha \cdot XAB. \quad (13)$$

$\alpha$  is a learnable neural network parameter, which can control the adaptation rate during the adversarial adaptation. In summary, we delineate the entire workflow of AdvLoRA in Algorithm 1.

---

**Algorithm 1** AdvLoRA WorkFlow on VLMs.

---

0: **Input:** Images:  $V = \{v_1, v_2, \dots, v_n\}$ ; Texts:  $W = \{w_1, w_2, \dots, w_n\}$ ; Visual encoder:  $\mathcal{F}_v$ ; Textual encoder:  $\mathcal{F}_w$ ; Pre-trained weight matrix:  $W_0$ ; LoRA matrix: **A, B**; Adaptive parameter:  $\alpha$ ; Restriction value:  $\epsilon$ ; PGD step:  $\xi$ ; Loss function:  $\mathcal{L}$ .

**Output:** Representations of  $V$  and  $W$ :  $Z^v = \{z_1^v, z_2^v, \dots, z_n^v\}$ ,  $Z^w = \{z_1^w, z_2^w, \dots, z_n^w\}$ .

**while** at adversarial fine-tuning stage **do**

    Perform clustering algorithm on  $W_0$  and obtain cluster center representation in Eq. (8) and Eq. (9);

    Obtain the LoRA matrix **A, B** from cluster center representation and  $W_0$  in Eq. (10) and Eq. (11);

    Impose constraints on **A** and **B** with SGD algorithm in Eq. (12);

    Calculate the loss  $l$  using  $V, W, Y, \mathcal{F}_v, \mathcal{F}_w$ , and the loss function  $\mathcal{L}$  in Eq. (5).

    Obtain the adversarial attack  $\delta$  with  $V, \epsilon, k, \xi$  and  $l$  in Eq. (3).

    Add  $\delta$  to original images  $V$  to obtain the attacked images  $V_\alpha$ .

    Update **A, B** via Eq. (4).

**end while**

Generate robust representations of  $V$  and  $W$  to downstream tasks with adversarially adapted **A, B** and  $\mathcal{F}_v, \mathcal{F}_w$ .

---

## 4 EXPERIMENT

### 4.1 Experimental Setup

**4.1.1 Datasets.** We comprehensively evaluated our proposed model, AdvLoRA, on two types of retrieval tasks and four commonly used datasets, to demonstrate the superior performance of AdvLoRA on cross-modal understanding tasks, including image-text retrieval: Flickr30K [120] and MSCOCO [118]; as well as video-text retrieval: DiDeMo [116] and MSRVT [122], More details can be seen in Appendix.

**4.1.2 Baselines.** We compare AdvLoRA with conventional adaptation methods, which are implemented by BLIP: full fine-tuning (BLIP-FFT), linear probe (BLIP-LP); as well as the PEFT method on BLIP: LoRA(BLIP-LoRA), Aurora, and Uniadapter. See more details in the Appendix.

**4.1.3 Metrics.** We employ  $Recall@k$  as our evaluation metric, where  $k$  denotes the number of entries considered within the top  $k$  retrieval results. This metric is expressed as a percentage.

**4.1.4 Implementations.** Our implementation is based on Salesforce’s open-source codebase [41]. Following [119, 121], we also apply BLIP [41] as our vision-language backbone for all tasks. We use PyTorch to implement all experiments on the NVIDIA V100

GPU (32G). For the video-text retrieval task, we follow the work of Wei et al. [101] by adopting an attack strategy that sparsely samples 20% of the video frames. Furthermore, we adopt the setup of BLIP, utilizing a momentum encoder to enhance the retrieval performance of our model. To ensure a fair comparison, the momentum encoder is also applied to the other baseline methods. We use AdamW [62] optimizer with weight decay. The rank of our proposed AdvLoRA is 10. Note that during the fine-tuning process, the parameters of the backbone model are kept frozen. More training details can be seen in the Appendix.

### 4.2 Vulnerability to Adversarial Attacks

In this section, we conduct adversarial attacks on BLIP and their variants adapted using PEFT methods to investigate their vulnerability to such attacks. Specifically, we perform PGD-3 attacks on the baseline model for two tasks across four datasets and then evaluate their performance under adversarial attacks. Figure 1 provides a simple illustration of the models’ vulnerability to adversarial attacks, while Table 1 and Table 2 present detailed data. The complete results on other datasets are provided in the Appendix. Through extensive experimentation, we draw a key conclusion as follows.

BLIP adapted by different methods are highly susceptible to adversarial perturbations. As Table 1 and Table 2 indicate, regardless of whether the method used is full fine-tuning or PEFT, performance degradation of 30.98% is observed. This phenomenon can be attributed to the inability of conventional VLMs and adaptation techniques to effectively learn semantically invariant features from the data.

### 4.3 Performance Comparisons

In this section, we conduct a comparative analysis between our proposed AdvLoRA and five baselines across two cross-modal retrieval tasks using four datasets. Specifically, we perform adversarial adaptation based on the PGD-3 [67] attack to all methods and then evaluate their performance under the condition of adversarial attack data and natural data.

Firstly, for image-text retrieval, we conducted experiments on adversarial attacked data for both Flickr30K and MSCOCO, as shown in Table 4 and Table 3. From these experiments, we draw two important conclusions as follows.

1) After adversarial adaptation, AdvLoRA outperforms all other baselines when faced with adversarial attacks. Notably, on MSCOCO, AdvLoRA surpasses all other PEFT methods by 12.17% and exceeds FFT by 2.47%, while using approximately 100x fewer tunable parameters than FFT.

2) AdvLoRA demonstrates enhanced adversarial robustness on larger datasets, highlighting the significant potential of PEFT methods in improving model robustness against adversarial attacks. Specifically, on the relatively smaller dataset Flickr30K, the performance of various baselines after adversarial adaptation is comparable and does not show a significant increase in robustness. However, on the larger dataset MSCOCO, FFT achieves considerable adversarial robustness, yet it still lags behind AdvLoRA. These results benefit not only from the design of AdvLoRA in terms of clustering parameterization and parameter alignment but also indicate that the effectiveness of adversarial adaptation improves with the increase of adaptation data.

**Table 1: Vulnerability experiment on MSCOCO. “FFT” and “LP” denoting full fine-tuning and linear probe. “Nat” and “Att” donate natural images and adversarially attacked images. “TR” and “IR” donate text-to-image retrieval and image-to-text retrieval.**

Method	Tunable Para.	MSCOCO TR				MSCOCO IR				Mean
		R@1	R@5	R@10	R@Mean	R@1	R@5	R@10	R@Mean	
BLIP+FFT+Nat	223M	80.46	95.40	97.64	91.17	63.25	85.54	91.49	80.09	85.63
BLIP+FFT+Att		53.38	75.12	82.62	70.37	42.25	67.03	76.47	61.92	
BLIP+LP+Nat	0.5M	72.30	91.10	95.22	86.21	56.96	80.75	87.85	75.19	80.70
BLIP+LP+Att		43.22	65.82	74.46	61.17	34.60	58.59	68.86	54.12	
BLIP+LoRA+Nat	2.8M	70.50	90.28	94.58	85.12	56.39	80.36	87.45	74.73	79.93
BLIP+LoRA+Att		43.20	66.20	74.80	61.40	35.85	60.40	70.16	55.47	
UniAdapter+Nat	19.5M	79.60	94.50	97.26	90.45	62.53	84.95	90.97	79.49	84.97
UniAdapter+Att		53.98	75.66	82.74	70.79	42.02	66.80	76.39	61.74	
Aurora+Nat	0.3M	78.00	93.40	96.66	89.35	61.45	83.95	90.39	78.60	83.98
Aurora+Att		44.56	67.04	75.00	62.20	34.98	59.34	68.75	54.36	

**Table 2: Vulnerability experiment on MSR-VTT. “TR” and “VR” donate text-to-video retrieval and video-to-text retrieval, respectively.**

Method	Tunable Para.	MSR-VTT TR				MSR-VTT VR				Mean
		R@1	R@5	R@10	R@Mean	R@1	R@5	R@10	R@Mean	
BLIP+FFT+Nat	223M	20.3	41.3	53.8	38.47	23.4	48.4	60.8	44.2	41.33
BLIP+FFT+Att		1.2	5	7.6	4.6	2.7	8.1	12.5	7.77	
BLIP+LP+Nat	0.5M	40.3	63.2	72.0	58.5	41.8	63.7	71.6	59.03	58.77
BLIP+LP+Att		7.7	16.1	20.1	14.63	14.4	26.4	32.8	24.53	
BLIP+LoRA+Nat	2.8M	47.2	71.4	80.5	66.36	45.8	70.7	80.3	65.6	65.98
BLIP+LoRA+Att		12.8	23.4	28.1	21.43	18.9	3.8	37.8	29.16	
UniAdapter+Nat	19.5M	42.4	68.4	77.4	62.73	42.9	68.4	78.3	63.2	62.97
UniAdapter+Att		8.3	15.4	18.9	14.2	11.6	22.6	27.2	20.47	
Aurora+Nat	0.3M	45.1	69.7	79.4	64.73	44.2	68.5	77.8	63.5	64.12
Aurora+Att		11.6	20.3	24.6	18.83	16.9	30.1	36.7	27.9	

**Table 3: Adversarial experiment on MSCOCO. An asterisk (\*) indicates that adversarial adaptation has been performed. The best results are displayed in bold, while the second-best results are underlined.**

Method	Tunable Para.	MSCOCO TR				MSCOCO IR				Mean
		R@1	R@5	R@10	R@Mean	R@1	R@5	R@10	R@Mean	
BLIP+FFT+Att	223M	53.38	75.12	82.62	70.37	42.25	67.03	76.47	61.92	66.15
BLIP+FFT*+Att	223M	<u>65.42</u>	<u>84.68</u>	89.4	<u>79.83</u>	<u>47.62</u>	<u>73.43</u>	<u>81.35</u>	<u>67.47</u>	<u>73.65</u>
BLIP+LoRA+Att	2.8M	43.2	66.2	74.8	61.4	35.85	60.4	70.16	55.47	58.44
BLIP+LoRA*+Att	2.8M	42.22	66.12	74.7	61.01	34.69	59.39	69.14	54.41	57.71
BLIP+LP+Att	0.5M	43.22	65.82	74.46	61.17	34.6	58.59	68.86	54.12	57.61
BLIP+LP*+Att	0.5M	44.14	67.18	76.04	62.45	34.57	59.14	69.3	54.34	58.40
UniAdapter+Att	19.5M	53.98	75.66	82.74	70.79	42.02	66.8	76.39	61.74	66.27
UniAdapter*+Att	19.5M	50.76	76.68	85.4	70.95	39.9	67.8	77.88	61.86	66.40
Aurora+Att	0.3M	44.56	67.04	75	62.2	34.98	59.34	68.75	54.36	58.28
Aurora*+Att	0.3M	54.56	77.68	84.52	72.25	40.08	60.17	75.66	60.17	65.64
AdvLoRA+Att	2.8M	46.76	69.18	76.72	64.22	37	61.25	70.76	56.34	60.28
AdvLoRA*+Att	2.8M	<b>67.28</b>	<b>87.16</b>	<b>92.76</b>	<b>82.4</b>	<b>49.02</b>	<b>75.88</b>	<b>84.59</b>	<b>69.83</b>	<b>76.12</b>

Secondly, for video-text retrieval, we conducted experiments on adversarial attacked data for both Didemo and MSR-VTT datasets, as shown in Table 6 and Table 5. From these experiments, we draw two conclusions from the image-text retrieval as follows.

1) AdvLoRA achieves excellent adversarial robustness on video data, surpassing all other baselines. In DiDeMo, AdvLoRA slightly

outperforms Uniadapter while using 7x fewer parameters. On MSR-VTT, AdvLoRA enhances the model’s adversarial robustness by 39.16% and significantly exceeds the other baselines.

2) AdvLoRA demonstrates better adversarial robustness on larger datasets. Specifically, on the relatively smaller dataset DiDeMo, the

**Table 4: Adversarial experiment on Flickr30K. An asterisk (\*) indicates that adversarial adaptation has been performed. The best results are displayed in bold, while the second-best results are underlined.**

Method	Tunable Para.	Flickr30K TR				Flickr30K IR				Mean
		R@1	R@5	R@10	R@Mean	R@1	R@5	R@10	R@Mean	
BLIP+FFT+Att	223M	21.1	38.4	46	35.16	21.96	42.62	51.18	38.58	36.87
BLIP+FFT*+Att	223M	64.6	84.8	87.7	79.03	55.06	79.52	84.46	<u>73.01</u>	76.02
BLIP+LoRA+Att	2.8M	67	81.8	84.2	77.67	<u>58.5</u>	77.48	82.7	72.89	75.28
BLIP+LoRA*+Att	2.8M	65.6	<b>87.1</b>	<u>89.5</u>	80.4	54.62	79.92	85.18	73.24	76.82
BLIP+LP+Att	0.5M	55.9	76	81.7	71.2	49.3	70.82	77.48	65.87	68.53
BLIP+LP*+Att	0.5M	56.1	75.7	82.7	71.5	48.14	70.5	78.18	65.61	68.55
UniAdapter+Att	19.5M	67.2	82.5	86.5	78.73	58.26	77.26	83.3	72.94	75.84
UniAdapter*+Att	19.5M	<b>71.2</b>	85.8	88.2	<u>81.73</u>	<b>59.12</b>	<b>80.4</b>	<u>85.82</u>	<b>75.11</b>	<u>78.42</u>
Aurora+Att	0.3M	65.4	80.7	84.4	76.83	56.98	76.64	82.22	71.95	74.39
Aurora*+Att	0.3M	69.1	84.1	87.3	80.17	56.8	78.82	83.76	73.13	77.15
AdvLoRA+Att	2.8M	66.2	82.5	85.8	78.17	57.7	77.52	83.32	72.85	75.51
AdvLoRA*+Att	2.8M	<u>71</u>	<u>86.8</u>	<b>90.7</b>	<b>82.83</b>	58.02	<u>80.1</u>	<b>85.9</b>	<u>74.67</u>	<b>78.75</b>

performance of various baselines after adversarial adaptation is comparable, and the robustness improvement is not significant. However, on the larger dataset MSR-VTT, the Uniadapter method achieves considerable adversarial robustness but is still inferior to AdvLoRA, and it uses 7x many parameters. Such results are attributed to the design of AdvLoRA in terms of clustering reparameterization and parameter alignment. It indicates that the effectiveness of adversarial adaptation improves with the increase of adaptation data.

Thirdly, we conducted experiments on natural data from four datasets, and Table 7 presents the results for MSCOCO. The complete results on other datasets are provided in the Appendix. From these experiments, we draw a significant conclusion as follows.

Adversarial adaptation can degrade the performance of the model on natural data. For instance, a comparison between Table 7 and Table 1 reveals that, except LP and LoRA, all other models experience a decline in performance after adversarial adaptation. However, the AdvLoRA method still achieves competitive results on MSCOCO. This can be attributed to AdvLoRA’s ability to learn semantically invariant feature representations. The reason for the lack of performance degradation in LP and LoRA may be due to their low sensitivity to adversarial adaptation, leading to an ineffective adaptation process. As shown in Table 3, LP and LoRA do not acquire improved adversarial robustness after adversarial adaptation.

#### 4.4 Ablation Study

In this section, we conduct an ablation study on AdvLoRA to demonstrate the effectiveness of the proposed clustering reparameterization, parameter alignment, and adaptive parameter update strategy on Didemo, and the results are presented in Figure 3. We draw the following conclusions.

The techniques proposed, including clustering reparameterization, parameter alignment, and adaptive parameter updates, are effective. Moreover, as evidenced by Figure 3, the model achieves optimal adversarial robustness when these methods are collectively employed.

#### 4.5 Adaptation Efficiency and Storage Cost

In this section, we conduct an analysis and comparison of the adaptation efficiency and storage cost associated with AdvLoRA. Table

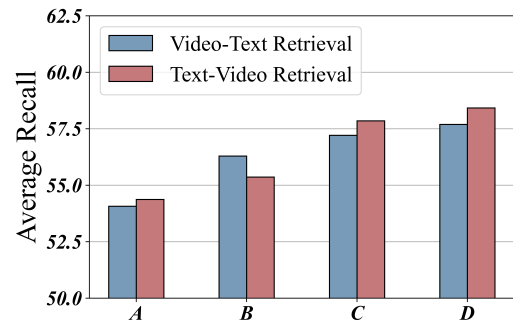


**Figure 3: Ablation study. A, B, C, D denotes LoRA, LoRA with parameter clustering, LoRA with parameter clustering and alignment, and AdvLoRA, respectively.**

8 illustrates the relative training GPU hours and GPU memory cost, where the time (or memory) of FFT is taken as one unit. The following conclusions can be drawn. 1) In terms of time overhead, AdvLoRA does not exhibit a pronounced advantage, but it outperforms Aurora and FFT. It is noteworthy that the adaptation process of models based on online weight decomposition, such as Aurora, requires more time than FFT. In contrast, AdvLoRA has a smaller time overhead due to the completion of only one offline clustering reparameterization and parameter alignment before adaptation. 2) In terms of memory overhead, AdvLoRA surpasses Aurora and FFT. Aurora again experiences a higher memory cost than FFT due to its heavier online decomposition. 3) Overall, AdvLoRA, without any additional constraints on training time and memory, can be considered an excellent adversarial adaptation method to enhance the adversarial robustness of VLMs.

#### 4.6 Hyperparameter Sensitivity Analysis

In this section, we conduct a sensitivity analysis on the rank size of AdvLoRA on Flickr30K. We set a series of values for the rank, namely 8, 10, 16, 32, and 64, and the results are presented in Figure 4 (a). AdvLoRA is not sensitive to the rank size, allowing us to

**Table 5: Adversarial experiment on MSR-VTT. An asterisk (\*) indicates that adversarial adaptation has been performed. The best results are displayed in bold, while the second-best results are underlined.**

Method	Tunable Para.	MSR-VTT TR				MSR-VTT VR				Mean
		R@1	R@5	R@10	R@Mean	R@1	R@5	R@10	R@Mean	
BLIP+FFT+Att	223M	1.2	5	7.6	4.6	2.7	8.1	12.5	7.77	6.18
BLIP+FFT*+Att	223M	21	41.9	50.8	37.9	21	46.8	57.9	41.9	39.9
BLIP+LoRA+Att	2.8M	12.8	23.4	28.1	21.43	18.9	30.8	37.8	29.16	25.30
BLIP+LoRA*+Att	2.8M	21.2	43.5	52.7	39.13	21	42.5	52.1	38.53	38.83
BLIP+LP+Att	0.5M	7.7	16.1	20.1	14.63	14.4	26.4	32.8	24.53	19.58
BLIP+LP*+Att	0.5M	14.5	26.8	33.3	24.87	15.8	26.7	33.5	25.33	25.10
UniAdapter+Att	19.5M	8.3	15.4	18.9	14.2	11.6	22.6	27.2	20.47	17.33
UniAdapter*+Att	19.5M	<u>38.6</u>	<u>64</u>	<u>74.5</u>	<u>59.03</u>	<u>39.2</u>	<u>64.9</u>	<u>75.8</u>	<u>59.97</u>	<u>59.50</u>
Aurora+Att	0.6M	11.6	20.3	24.6	18.83	16.9	30.1	36.7	27.9	23.37
Aurora*+Att	0.6M	38.1	63.6	73.5	58.4	37	60.8	72.7	56.83	57.62
AdvLoRA+Att	2.8M	12.3	21.8	26.2	20.1	15.8	28.4	34.2	26.13	23.12
AdvLoRA*+Att	2.8M	<b>40.4</b>	<b>67.4</b>	<b>78.6</b>	<b>62.13</b>	<b>40.5</b>	<b>68.4</b>	<b>78.4</b>	<b>62.43</b>	<b>62.28</b>

**Table 6: Adversarial experiment on Didemo. An asterisk (\*) indicates that adversarial adaptation has been performed. The best results are displayed in bold, while the second-best results are underlined.**

Method	Tunable Para.	Didemo TR				Didemo VR				Mean
		R@1	R@5	R@10	R@Mean	R@1	R@5	R@10	R@Mean	
BLIP+FFT+Att	223M	12.66	26.32	35.39	24.79	14.56	31.7	40.58	28.95	26.87
BLIP+FFT*+Att	223M	29.71	53.04	64.3	49.08	31.21	55.63	67.4	51.41	50.25
BLIP+LoRA+Att	2.8M	33.2	57.43	66.7	52.44	32.7	56.73	68.1	52.51	52.48
BLIP+LoRA*+Att	2.8M	33.7	59.82	69.59	54.37	32.8	59.02	70.39	54.07	54.22
BLIP+LP+Att	0.5M	23.13	45.86	53.54	40.84	26.02	47.06	57.03	43.37	42.11
BLIP+LP*+Att	0.5M	22.73	45.46	54.04	40.74	25.32	46.46	56.73	42.84	41.79
UniAdapter+Att	19.5M	27.02	52.14	64.01	47.72	9.27	24.83	36.69	23.6	35.66
UniAdapter*+Att	19.5M	<u>36.38</u>	<u>63.5</u>	<b>73.57</b>	<u>57.82</u>	35.88	<b>64.3</b>	<b>73.87</b>	<b>58.02</b>	<u>57.92</u>
Aurora+Att	0.6M	30.31	52.94	64.11	49.12	31.21	54.74	64.61	50.19	49.65
Aurora*+Att	0.6M	35.59	61.22	72.18	56.33	<u>36.69</u>	62.01	71.88	56.86	56.60
AdvLoRA+Att	2.8M	34.4	62.11	71.39	55.97	35.19	62.81	70.99	56.33	56.15
AdvLoRA*+Att	2.8M	<b>37.38</b>	<b>64.4</b>	<u>73.48</u>	<b>58.42</b>	<b>36.99</b>	<u>63.21</u>	<u>72.88</u>	<u>57.69</u>	<b>58.06</b>

**Table 7: Natural experiment with adversarial adaptation on MSCOCO. “Nat” donates natural images. An asterisk (\*) indicates that adversarial adaptation has been performed.**

Method	Tunable Para.	MSCOCO TR				MSCOCO IR				Mean
		R@1	R@5	R@10	R@Mean	R@1	R@5	R@10	R@Mean	
BLIP+FFT*+Nat	223M	57.28	78.92	86.36	74.17	48.52	75.04	83.77	69.11	71.65
BLIP+LoRA*+Nat	2.8M	70.76	90.44	94.68	85.29	56.39	80.38	87.48	74.75	80.02
BLIP+LP*+Nat	0.5M	72.58	91.2	95.22	86.33	57.15	80.93	88.05	75.38	80.86
UniAdapter*+Nat	19.5M	55.62	81.24	89.02	75.29	45.06	72.99	82.61	66.89	71.09
Aurora*+Nat	0.3M	70.92	89.39	93.94	84.74	54.38	79.38	86.88	73.54	79.15
AdvLoRA*+Nat	2.8M	70.58	90.42	94.54	85.18	56.36	80.35	87.29	74.67	79.92

select an appropriate rank according to our needs to reduce the cost of adaptation.

#### 4.7 Loss Convergence Analysis

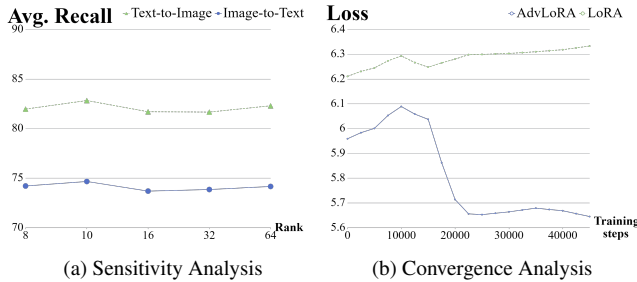
In this section, we conduct a convergence analysis experiment between AdvLoRA and LoRA on Flickr30K. The results are presented in Figure 4 (b). Analysis of the experimental results we can draw

the following conclusion. 1) AdvLoRA demonstrates superior convergence over LoRA in the adversarial adaptation process, achieving a significantly reduced loss level. 2) AdvLoRA accelerates the convergence of adversarial adaptation more effectively than LoRA. These efficiencies and effectiveness can be attributed to the design of clustering reparameterization, parameter alignment, and adaptive parameter update strategy.



**Table 8: Comparison on the training time and GPU memory.**

Method	Tunable Para.	Time	Mem.
BLIP+FFT	223M	1.00	1.00
BLIP+LoRA	2.8M	0.91	0.85
BLIP+LP	0.5M	0.79	0.67
Uniadapter	19.5M	0.93	0.77
Aurora	0.3M	1.05	1.04
AdvLoRA	2.8M	0.94	0.85

**Figure 4: Analysis experiments of our proposed method**

## 5 CONCLUSION

In this paper, we aim to alleviate the security risks in the Vision-Language Models (VLMs). First of all, we show the vulnerability of VLMs with various adaptation methods under adversarial attacks via extensive experiments. Besides, as the sizes of VLMs increase, simply applying the conventional adversarial adaptation methods to VLMs easily leads to 1) unpromising adversarial robustness and 2) tremendous parameter and training costs. From these motivations, a novel parameter-efficient adversarial adaptation method named AdvLoRA is proposed with parameter clustering, parameter alignment, and adaptive parameter update. Extensive experiments demonstrate the effectiveness and efficiency of AdvLoRA. This result reveals the intrinsic low-rank property that emerges during the adversarial adaptation process. Our proposed technique, which involves clustering reparameterization and parameter alignment, has been instrumental in facilitating the adaptation process. We have thereby offered a novel perspective for researchers in the field of security within the broader context of AGI.

However, in this paper, we merely use the simple PCD-3 for the adversarial attacks. In the future, it is worth adopting more challenging attacks and further optimizing the memory and computational budget during the adaptation process.

## ACKNOWLEDGMENTS

This work is supported by the Ministry of Science and Technology of China under Grant No. 2020AAA0108401, and the Natural Science Foundation of China under Grant Nos. 72225011 and 72293575. Note that Xiaolong Zheng is the corresponding author of this article.

## A DATASETS

- **Flickr30K** [120] contains 31,783 images and 158,915 captions totally. Each image is often annotated with 5 captions. Following the split in Uniadapter [119] and Aurora [121], we

use 1,000 images for testing, another 1,000 for validation, and the rest for training.

- **MSCOCO** [118] is a large dataset containing 123,287 images and 616,435 captions. Each image is annotated with 5 captions. Following the split in Uniadapter [119] and Aurora [121], we use 5,000 images for testing, another 5,000 for validation, and the rest for training.
- **Didemo** [116] contains 10,000 videos and 40,000 annotations. Following Frozen in Time [117], we concatenate all descriptions corresponding to the same video into a single sentence to conduct actually video-paragraph retrieval task.
- **MSR-VTT** [122] is a popular video-text dataset. It contains 10,000 video and 200,000 captions. Following the split in Uniadapter [119] and Aurora [121], we use 1,000 videos for testing, another 9,000 for training.

## B BASELINES

- **BLIP-FFT** is a conventional adaptation technique that enhances the performance of BLIP for specific downstream tasks by retraining and updating full parameters in downstream tasks.
- **BLIP-LP** is an adaptation technique that involves adding and training a linear layer on top of the frozen pre-trained model BLIP to adapt to specific downstream tasks.
- **BLIP-LoRA** is a Parameter-Efficient Fine-Tuning (PEFT) technology that adapts BLIP by introducing low-rank adapters to capture task-specific information, allowing for efficient adaptation to downstream tasks with minimal tunable parameter updates.
- **Uniadapter** [119] is the first adapter-based PEFT technology for parameter-efficient cross-modal adaptation.
- **Aurora** [121] is a parameter-efficient cross-modal transfer learning framework that uses mode approximation to generate a minimal set of tunable parameters, achieving lightweight multi-modal adaptation.

## C HYPERPARAMETER SETTING

We present the hyperparameter setting in Table 9.

## D VULNERABILITY TO ADVERSARIAL ATTACKS

In this section, we present the vulnerability results on Flickr30K and DiDeMo in Table 10 and Table 11. We have the conclusion that BLIP adapted by different methods are highly susceptible to adversarial perturbations, which is similar to that in the main text.

## E PERFORMANCE ON NATURAL DATA

In this section, we present the performance results of natural data on Flickr30K, DiDeMo and MSR-VTT in Table 12, Table 13 and Table 14. We have the following conclusion similar to that in the main text.

Adversarial adaptation can degrade the performance of the model on natural data. However, the AdvLoRA method still achieves competitive results on these datasets. This can be attributed to AdvLoRA’s ability to learn semantically invariant feature representations. The reason for the lack of performance degradation in LP and

**Table 9: Hyperparameter setting**

config	Image-text Retrieval		Video-text Retrieval	
	Flickr30K	MSCOCO	Didemo	MSR-VTT
optimizer	AdamW	AdamW	AdamW	AdamW
learning rate	1e-5	1e-5	1e-4	1e-4
schedule	cosine decay	cosine decay	cosine decay	cosine decay
training batchsize	16	16	8	8
inference batchsize	32	32	8	8
frames	-	-	16	16
attack ratio	-	-	20%	20%
epochs	5	5	5	5
training input	384	384	8*224	8*224
inference input	384	384	16*224	16*224
adversarial type	PGD-3	PGD-3	PGD-3	PGD-3
attack alpha	1/255	1/255	1/255	1/255
PGD-epsilon	1/255	1/255	1/255	1/255
rank	10	10	10	10
adaptive weight	1e-3	1e-3	1e-3	1e-3
weight norm learning rate	1e-3	1e-3	1e-3	1e-3

**Table 10: Vulnerability experiment on Flickr30K. “FFT” and “LP” denoting full fine-tuning and linear probe. “Nat” and “Att” donate natural images and adversarially attacked images. “TR” and “IR” donate text-to-image retrieval and image-to-text retrieval.**

Method	Tunable Para.	Flickr30K TR				Flickr30K IR				Mean
		R@1	R@5	R@10	R@Mean	R@1	R@5	R@10	R@Mean	
BLIP+FFT+Nat	223M	72.8	90.8	95.5	86.37	63.4	86.58	92	80.66	83.52
BLIP+FFT+Att		21.1	38.4	46	35.16	21.96	42.62	51.68	38.58	36.87(-46.65%)
BLIP+LP+Nat	0.5M	89	98.5	99.5	95.67	78.32	94.34	96.98	89.88	92.78
BLIP+LP+Att		55.9	76	81.7	71.2	49.3	70.82	77.48	65.87	68.54(-24.24%)
BLIP+LoRA+Nat	2.8M	87	98.1	99.5	94.87	72.9	93.9	96.84	87.88	91.38
BLIP+LoRA+Att		71.6	92.1	95.5	86.4	60.62	85.92	91.18	79.24	82.82(-8.56%)
UniAdapter+Nat	19.5M	96.7	99.7	100	98.8	86.18	97.34	98.82	94.11	96.46
UniAdapter+Att		70.2	85.5	89.5	81.73	61.26	80.26	86.3	75.94	78.84(-17.62%)
Aurora+Nat	0.3M	96.7	99.8	100	98.83	85.76	97.24	98.72	93.91	96.37
Aurora+Att		69.4	84.7	88.4	80.83	60.98	80.64	86.22	75.95	78.39(-17.98%)

**Table 11: Vulnerability experiment on Didemo. “TR” and “VR” donate text-to-video retrieval and video-to-text retrieval, respectively.**

Method	Tunable Para.	Didemo TR				Didemo VR				Mean
		R@1	R@5	R@10	R@Mean	R@1	R@5	R@10	R@Mean	
BLIP+FFT+Nat	223M	30.51	55.63	66.4	50.85	32.8	58.52	68.49	53.27	52.06
BLIP+FFT+Att		12.66	26.32	35.39	24.79	14.56	31.7	40.58	28.95	26.87(-25.19%)
BLIP+LP+Nat	0.5M	25.32	44.77	53.24	41.11	26.82	50.25	58.42	45.16	43.14
BLIP+LP+Att		23.13	45.86	53.54	40.84	26.02	47.06	57.03	43.37	42.11(-1.03%)
BLIP+LoRA+Nat	2.8M	36.79	63.21	72.28	57.43	34.1	62.41	73.08	56.53	56.98
BLIP+LoRA+Att		33.2	57.43	66.7	52.44	32.7	56.73	68.1	52.51	52.48(-4.51%)
UniAdapter+Nat	19.5M	32.8	60.02	71.19	54.67	9.97	28.32	40.38	26.22	40.45
UniAdapter+Att		27.02	52.14	64.01	47.72	9.27	24.83	36.69	23.6	35.66(-4.79%)
Aurora+Nat	0.3M	35.59	63.61	73.08	57.43	37.49	63.01	72.68	57.73	57.58
Aurora+Att		30.31	52.94	64.11	49.12	31.21	54.74	64.61	50.19	49.66(-7.92%)

LoRA may be due to their low sensitivity to adversarial adaptation, leading to an ineffective adaptation process.

**Table 12: Natural experiment with adversarial adaptation on Flickr30K. “Nat” donates natural images. An asterisk (\*) indicates that adversarial adaptation has been performed. The best results are displayed in bold, while the second-best results are underlined.**

Method	Tunable Para.	Flickr30K TR				Flickr30K IR				Mean
		R@1	R@5	R@10	R@Mean	R@1	R@5	R@10	R@Mean	
BLIP+FFT+Nat	223M	72.8	90.8	95.5	86.37	63.4	86.58	92	80.66	83.51
BLIP+LoRA+Nat	2.8M	<b>96.9</b>	<b>99.9</b>	<b>100</b>	<b>98.93</b>	<b>86.72</b>	<b>97.78</b>	<b>98.82</b>	<b>94.44</b>	<b>96.69</b>
BLIP+LB+Nat	0.5M	89	98.5	<u>99.5</u>	95.67	78.32	94.34	96.98	89.88	92.77
UniAdapter+Nat	19.5M	<u>96.7</u>	<u>99.7</u>	<b>100</b>	98.8	<u>86.18</u>	<u>97.34</u>	<b>98.82</b>	<u>94.11</u>	<u>96.46</u>
Aurora+Nat	0.3M	<u>96.7</u>	<u>99.8</u>	<b>100</b>	<u>98.83</u>	<u>85.76</u>	<u>97.24</u>	<u>98.72</u>	93.91	96.37
AdvLoRA+Nat	2.8M	96	99.7	<b>100</b>	98.57	85.68	97	98.64	93.77	96.17

**Table 13: Natural experiment with adversarial adaptation on Didemo. “Nat” donates natural videos. An asterisk (\*) indicates that adversarial adaptation has been performed. The best results are displayed in bold, while the second-best results are underlined.**

Method	Tunable Para.	Didemo TR				Didemo VR				Mean
		R@1	R@5	R@10	R@Mean	R@1	R@5	R@10	R@Mean	
BLIP+FFT+Nat	223M	30.51	55.63	66.4	50.85	32.8	58.52	68.49	53.27	52.06
BLIP+LoRA+Nat	2.8M	<b>36.79</b>	<u>63.21</u>	<u>72.28</u>	<b>57.43</b>	34.1	<u>62.41</u>	<b>73.08</b>	<u>56.53</u>	<u>56.98</u>
BLIP+LB+Nat	0.5M	25.32	<u>44.77</u>	<u>53.24</u>	41.11	26.82	50.25	58.42	45.16	43.14
UniAdapter+Nat	19.5M	32.8	60.02	71.19	<u>54.67</u>	9.97	28.32	40.38	26.22	40.45
Aurora+Nat	0.6M	<u>35.59</u>	<b>63.61</b>	<b>73.08</b>	<b>57.43</b>	<b>37.49</b>	<b>63.01</b>	<u>72.68</u>	<b>57.73</b>	<b>57.58</b>
AdvLoRA+Nat	2.8M	32.1	60.72	69.39	54.07	<u>35.29</u>	59.82	71.18	55.43	54.75

**Table 14: Natural experiment with adversarial adaptation on MSR-VTT. “Nat” donates natural images. An asterisk (\*) indicates that adversarial adaptation has been performed. The best results are displayed in bold, while the second-best results are underlined.**

Method	Tunable Para.	MSR-VTT TR				MSR-VTT VR				Mean
		R@1	R@5	R@10	R@Mean	R@1	R@5	R@10	R@Mean	
BLIP+FFT+Nat	223M	20.3	41.3	53.8	38.47	23.4	48.4	60.8	44.2	41.33
BLIP+LoRA+Nat	2.8M	<b>47.2</b>	<u>71.4</u>	<u>80.5</u>	<u>66.36</u>	<u>45.8</u>	<u>70.7</u>	<b>80.3</b>	<u>65.6</u>	<u>65.98</u>
BLIP+LB+Nat	0.5M	40.3	63.2	72.0	58.5	41.8	63.7	71.6	59.03	58.77
UniAdapter+Nat	19.5M	42.4	68.4	77.4	62.73	42.9	68.4	78.3	63.2	62.97
Aurora+Nat	0.6M	45.1	69.7	79.4	64.73	44.2	68.5	77.8	63.5	64.12
AdvLoRA+Nat	2.8M	<u>47.1</u>	<b>71.8</b>	<b>81.9</b>	<b>66.93</b>	<b>47.5</b>	<b>71.2</b>	<u>79.9</u>	<b>66.2</b>	<b>66.57</b>

## F CASE STUDY

In this section, we conduct a case study on MSR-VTT, as illustrated in Figure 5. It can be observed that AdvLoRA achieves robust retrieval performance under adversarial attacks.

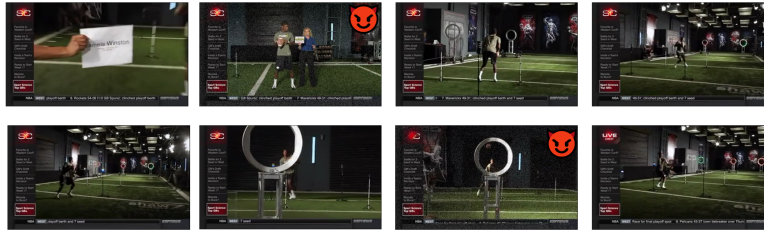
## REFERENCES

- [1] Josh Achiam, Steven Adler, Sandhini Agarwal, Lama Ahmad, Ilge Akkaya, Florencia Leoni Aleman, Diogo Almeida, Janko Altschmidt, Sam Altman, Shyamal Anadkat, et al. 2023. Gpt-4 technical report. *arXiv preprint arXiv:2303.08774* (2023).
- [2] Charu C Aggarwal and ChengXiang Zhai. 2012. A survey of text clustering algorithms. *Mining text data* (2012).
- [3] Ahmed Agiza, Marina Neseem, and Sherief Reda. 2024. MTLORA: A Low-Rank Adaptation Approach for Efficient Multi-Task Learning. *arXiv preprint arXiv:2403.20320* (2024).
- [4] Jean-Baptiste Alayrac, Jeff Donahue, Pauline Luc, Antoine Miech, Iain Barr, Yana Hasson, Karel Lenc, Arthur Mensch, Katherine Millican, Malcolm Reynolds, et al. 2022. Flamingo: a visual language model for few-shot learning. *Proc. of NeurIPS* (2022).
- [5] Lisa Anne Hendricks, Oliver Wang, Eli Shechtman, Josef Sivic, Trevor Darrell, and Bryan Russell. 2017. Localizing moments in video with natural language. In *Proc. of ICCV*.
- [6] YM Asano, C Rupprecht, and A Vedaldi. 2019. Self-labelling via simultaneous clustering and representation learning. In *Proc. of ICLR*.
- [7] Hyojin Bahng, Ali Jahani, Swami Sankaranarayanan, and Phillip Isola. 2022. Exploring visual prompts for adapting large-scale models. *arXiv preprint arXiv:2203.17274* (2022).
- [8] Jinze Bai, Shuai Bai, Shusheng Yang, Shijie Wang, Sinan Tan, Peng Wang, Junyang Lin, Chang Zhou, and Jingren Zhou. 2023. Qwen-vl: A frontier large vision-language model with versatile abilities. *arXiv preprint arXiv:2308.12966* (2023).
- [9] Fan Bao, Shen Nie, Kaiwen Xue, Chongxuan Li, Shi Pu, Yaole Wang, Gang Yue, Yue Cao, Hang Su, and Jun Zhu. 2023. One transformer fits all distributions in multi-modal diffusion at scale. *arXiv preprint arXiv:2303.06555* (2023).
- [10] Yichao Cai, Yuhang Liu, Zhen Zhang, and Javen Qinfeng Shi. 2023. CLAP: Contrastive Learning with Augmented Prompts for Robustness on Pretrained Vision-Language Models. *arXiv preprint arXiv:2311.16445* (2023).
- [11] Mathilde Caron, Piotr Bojanowski, Armand Joulin, and Matthijs Douze. 2018. Deep clustering for unsupervised learning of visual features. In *Proc. of ECCV*.
- [12] Mathilde Caron, Ishan Misra, Julien Mairal, Priya Goyal, Piotr Bojanowski, and Armand Joulin. 2020. Unsupervised learning of visual features by contrasting cluster assignments. *Proc. of NeurIPS* (2020).
- [13] Mathilde Caron, Hugo Touvron, Ishan Misra, Hervé Jégou, Julien Mairal, Piotr Bojanowski, and Armand Joulin. 2021. Emerging properties in self-supervised vision transformers. In *Proc. of ICCV*.
- [14] Yen-Chun Chen, Linjie Li, Licheng Yu, Ahmed El Kholy, Faisal Ahmed, Zhe Gan, Yu Cheng, and Jingjing Liu. 2020. Uniter: Universal image-text representation learning. In *Proc. of ECCV*.
- [15] Wei Dai, Jicong Fan, Yiming Miao, and Kai Hwang. 2023. Deep Learning Model Compression With Rank Reduction in Tensor Decomposition. *IEEE*

Video7168:

AdvLoRA retrieval result: He is playing with ball

Aurora retrieval result: Some people video conferencing as they watch a movie



Video8915:

AdvLoRA retrieval result: Person cooking up somefood

Aurora retrieval result: A women preparing a duck to roast



Video8128:

AdvLoRA retrieval result: A cartoon character prepares to ride a bicycle

Aurora retrieval result: People are walking down a street holding signs



(a) Positive Sample Pairs

**Figure 5: Case study of MSR-VTT. We sample and visualize eight frames from the videos. The frames with the devil denote that they are under the adversarial attacks. The first and second texts are the output of AdvLoRA and Aurora, respectively.**

*Transactions on Neural Networks and Learning Systems* (2023).

- [16] Tim Dettmers, Artidoro Pagnoni, Ari Holtzman, and Luke Zettlemoyer. 2023. Qlora: Efficient finetuning of quantized llms. *arXiv preprint arXiv:2305.14314* (2023).
- [17] Jacob Devlin, Ming-Wei Chang, Kenton Lee, and Kristina Toutanova. 2018. Bert: Pre-training of deep bidirectional transformers for language understanding. *arXiv preprint arXiv:1810.04805* (2018).
- [18] Shihan Dou, Enyu Zhou, Yan Liu, Songyang Gao, Jun Zhao, Wei Shen, Yuhao Zhou, Zhiheng Xi, Xiao Wang, Xiaoran Fan, et al. 2023. Loramoe: Revolutionizing mixture of experts for maintaining world knowledge in language model alignment. *arXiv preprint arXiv:2312.09979* (2023).
- [19] Martin Ester, Hans-Peter Kriegel, Jörg Sander, Xiaowei Xu, et al. 1996. A density-based algorithm for discovering clusters in large spatial databases with noise. In *Proc. of KDD*.
- [20] Nanyi Fei, Zhiwu Lu, Yizhao Gao, Guoxing Yang, Yuqi Huo, Jingyuan Wen, Haoyu Lu, Ruihua Song, Xin Gao, Tao Xiang, et al. 2022. Towards artificial general intelligence via a multimodal foundation model. *Nature Communications* (2022).
- [21] Shuo Feng, Xintao Yan, Haowei Sun, Yiheng Feng, and Henry X Liu. 2021. Intelligent driving intelligence test for autonomous vehicles with naturalistic and adversarial environment. *Nature communications* (2021).
- [22] Samuel G Finlayson, John D Bowers, Joichi Ito, Jonathan L Zittrain, Andrew L Beam, and Isaac S Kohane. 2019. Adversarial attacks on medical machine learning. *Science* (2019).
- [23] Zhe Gan, Yen-Chun Chen, Linjie Li, Chen Zhu, Yu Cheng, and Jingjing Liu. 2020. Large-scale adversarial training for vision-and-language representation learning. *Proc. of NeurIPS* (2020).
- [24] Peng Gao, Shijie Geng, Renrui Zhang, Teli Ma, Rongyao Fang, Yongfeng Zhang, Hongsheng Li, and Yu Qiao. 2023. Clip-adapter: Better vision-language models with feature adapters. *International Journal of Computer Vision* (2023).
- [25] Gregor Geigle, Jonas Pfeiffer, Nils Reimers, Ivan Vulić, and Iryna Gurevych. 2022. Retrieve fast, rerank smart: Cooperative and joint approaches for improved cross-modal retrieval. *TACL* (2022).
- [26] Ross Girshick. 2015. Fast r-cnn. In *Proc. of ICCV*.
- [27] Ben Goertzel. 2014. Artificial general intelligence: concept, state of the art, and future prospects. *Journal of Artificial General Intelligence* (2014).
- [28] Ian J Goodfellow, Jonathon Shlens, and Christian Szegedy. 2014. Explaining and harnessing adversarial examples. *arXiv preprint arXiv:1412.6572* (2014).
- [29] Xifeng Guo, Long Gao, Xinwang Liu, and Jianping Yin. 2017. Improved Deep Embedded Clustering with Local Structure Preservation. In *Proc. of IJCAI*.
- [30] John A Hartigan and Manchek A Wong. 1979. Algorithm AS 136: A k-means clustering algorithm. *Journal of the royal statistical society. series c (applied statistics)* (1979).

- [31] Soufiane Hayou, Nikhil Ghosh, and Bin Yu. 2024. LoRA+: Efficient Low Rank Adaptation of Large Models. *arXiv preprint arXiv:2402.12354* (2024).
- [32] Neil Houlsby, Andrei Giurgiu, Stanislaw Jastrzebski, Bruna Morrone, Quentin De Laroussilhe, Andrea Gesmundo, Mona Attariyan, and Sylvain Gelly. 2019. Parameter-efficient transfer learning for NLP. In *Proc. of ICML*.
- [33] Edward J Hu, Yelong Shen, Phillip Wallis, Zeyuan Allen-Zhu, Yuanzhi Li, Shean Wang, Lu Wang, and Weizhu Chen. 2021. Lora: Low-rank adaptation of large language models. *arXiv preprint arXiv:2106.09685* (2021).
- [34] Siteng Huang, Biao Gong, Yulin Pan, Jianwen Jiang, Yiliang Lv, Yuyuan Li, and Donglin Wang. 2023. VoP: Text-Video Co-operative Prompt Tuning for Cross-Modal Retrieval. In *Proc. of CVPR*.
- [35] Zhicheng Huang, Zhaoyang Zeng, Bei Liu, Dongmei Fu, and Jianlong Fu. 2020. Pixel-bert: Aligning image pixels with text by deep multi-modal transformers. *arXiv preprint arXiv:2004.00849* (2020).
- [36] Karwan Jacksi, Rowaida Kh Ibrahim, Subhi RM Zeebaree, Rizgar R Zebari, and Mohammed AM Sadeeq. 2020. Clustering documents based on semantic similarity using HAC and K-mean algorithms. In *2020 International Conference on Advanced Science and Engineering (ICOASE)*.
- [37] Menglin Jia, Luming Tang, Bor-Chun Chen, Claire Cardie, Serge Belongie, Bharath Hariharan, and Ser-Nam Lim. 2022. Visual prompt tuning. In *Proc. of ECCV*.
- [38] Wonjae Kim, Bokyung Son, and Ildoo Kim. 2021. Vilt: Vision-and-language transformer without convolution or region supervision. In *Proc. of ICML*.
- [39] Yann LeCun, Léon Bottou, Yoshua Bengio, and Patrick Haffner. 1998. Gradient-based learning applied to document recognition. *Proc. IEEE* (1998).
- [40] Junnan Li, Dongxu Li, Silvio Savarese, and Steven Hoi. 2023. Blip-2: Bootstrapping language-image pre-training with frozen image encoders and large language models. In *Proc. of ICML*.
- [41] Junnan Li, Dongxu Li, Caiming Xiong, and Steven Hoi. 2022. Blip: Bootstrapping language-image pre-training for unified vision-language understanding and generation. In *Proc. of ICML*.
- [42] Junnan Li, Ramprasaath Selvaraju, Akhilesh Gotmare, Shafiq Joty, Caiming Xiong, and Steven Chu Hong Hoi. 2021. Align before fuse: Vision and language representation learning with momentum distillation. *Proc. of NeurIPS* (2021).
- [43] Junnan Li, Pan Zhou, Caiming Xiong, and Steven Hoi. 2020. Prototypical Contrastive Learning of Unsupervised Representations. In *Proc. of ICLR*.
- [44] Linjie Li, Zhe Gan, and Jingjing Liu. 2020. A closer look at the robustness of vision-and-language pre-trained models. *arXiv preprint arXiv:2012.08673* (2020).
- [45] Xiang Lisa Li and Percy Liang. 2021. Prefix-tuning: Optimizing continuous prompts for generation. *arXiv preprint arXiv:2101.00190* (2021).
- [46] Yunfan Li, Peng Hu, Zitao Liu, Dezhong Peng, Joey Tianyi Zhou, and Xi Peng. 2021. Contrastive clustering. In *Proc. of AAAI*.
- [118] Tsung-Yi Lin, Michael Maire, Serge Belongie, James Hays, Pietro Perona, Deva Ramanan, Piotr Dollár, and C Lawrence Zitnick. 2014. Microsoft coco: Common objects in context. In *Proc. of ECCV*.
- [48] Haotian Liu, Chunyuan Li, Yuheng Li, and Yong Jae Lee. 2023. Improved baselines with visual instruction tuning. *arXiv preprint arXiv:2310.03744* (2023).
- [49] Haotian Liu, Chunyuan Li, Qingyang Wu, and Yong Jae Lee. 2024. Visual instruction tuning. *Proc. of NeurIPS* (2024).
- [50] Ninghao Liu, Hongxia Yang, and Xia Hu. 2018. Adversarial detection with model interpretation. In *Proc. of KDD*.
- [51] Quande Liu, Youpeng Wen, Jianhua Han, Chunjing Xu, Hang Xu, and Xiaodan Liang. 2022. Open-world semantic segmentation via contrasting and clustering vision-language embedding. In *Proc. of ECCV*.
- [52] Xiaodong Liu, Hao Cheng, Pengcheng He, Weizhu Chen, Yu Wang, Hoifung Poon, and Jianfeng Gao. 2020. Dezsarial training for large neural language models. *arXiv preprint arXiv:2004.08994* (2020).
- [53] Xiao Liu, Yanan Zheng, Zhengxiao Du, Ming Ding, Yujie Qian, Zhilin Yang, and Jie Tang. 2023. GPT understands, too. *AI Open* (2023).
- [54] Yue Liu, Ke Liang, Jun Xia, Sihang Zhou, Xihong Yang, Xinwang Liu, and Stan Z Li. 2023. Dink-net: Neural clustering on large graphs. *arXiv preprint arXiv:2305.18405* (2023).
- [55] Yue Liu, Wenxuan Tu, Sihang Zhou, Xinwang Liu, Linxuan Song, Xihong Yang, and En Zhu. 2022. Deep graph clustering via dual correlation reduction. In *Proc. of AAAI*.
- [56] Yue Liu, Jun Xia, Sihang Zhou, Xihong Yang, Ke Liang, Chenchen Fan, Yan Zhuang, Stan Z Li, Xinwang Liu, and Kunlun He. 2022. A Survey of Deep Graph Clustering: Taxonomy, Challenge, Application, and Open Resource. *arXiv preprint arXiv:2211.12875* (2022).
- [57] Yue Liu, Xihong Yang, Sihang Zhou, Xinwang Liu, Siwei Wang, Ke Liang, Wenxuan Tu, and Liang Li. 2023. Simple contrastive graph clustering. *IEEE Transactions on Neural Networks and Learning Systems* (2023).
- [58] Yue Liu, Xihong Yang, Sihang Zhou, Xinwang Liu, Zhen Wang, Ke Liang, Wenxuan Tu, Liang Li, Jingcan Duan, and Cancan Chen. 2023. Hard sample aware network for contrastive deep graph clustering. In *Proc. of AAAI*.
- [59] Yue Liu, Sihang Zhou, Xinwang Liu, Wenxuan Tu, and Xihong Yang. 2022. Improved dual correlation reduction network. *arXiv preprint arXiv:2202.12533* (2022).
- [60] Yue Liu, Shihao Zhu, Jun Xia, Yingwei Ma, Jian Ma, Wenliang Zhong, Guannan Zhang, Kejun Zhang, and Xinwang Liu. 2024. End-to-end Learnable Clustering for Intent Learning in Recommendation. *arXiv preprint arXiv:2401.05975* (2024).
- [61] Zeyu Liu, Souvik Kundu, Anni Li, Junrui Wan, Lianghao Jiang, and Peter Anthony Beerel. 2024. AFLoRA: Adaptive Freezing of Low Rank Adaptation in Parameter Efficient Fine-Tuning of Large Models. *arXiv preprint arXiv:2403.13269* (2024).
- [62] Ilya Loshchilov and Frank Hutter. 2018. Decoupled Weight Decay Regularization. In *Proc. of ICML*.
- [119] Haoyu Lu, Mingyu Ding, Yuqi Huo, Guoxing Yang, Zhiwu Lu, Masayoshi Tomizuka, and Wei Zhan. 2023. UniAdapter: Unified Parameter-Efficient Transfer Learning for Cross-modal Modeling. *arXiv preprint arXiv:2302.06605* (2023).
- [64] Jiaseen Lu, Dhruv Batra, Devi Parikh, and Stefan Lee. 2019. Vlbart: Pretraining task-agnostic visiolinguistic representations for vision-and-language tasks. *Proc. of NeurIPS* (2019).
- [65] Yuning Lu, Jianzhuang Liu, Yonggang Zhang, Yajing Liu, and Xinmei Tian. 2022. Prompt distribution learning. In *Proc. of CVPR*.
- [66] Xingjun Ma, Yuhao Niu, Lin Gu, Yisen Wang, Yitian Zhao, James Bailey, and Feng Lu. 2021. Understanding adversarial attacks on deep learning based medical image analysis systems. *Pattern Recognition* (2021).
- [67] Aleksander Madry, Aleksandar Makelov, Ludwig Schmidt, Dimitris Tsipras, and Adrian Vladu. 2018. Towards Deep Learning Models Resistant to Adversarial Attacks. In *Proc. of ICLR*.
- [68] Chengzhi Mao, Scott Geng, Junfeng Yang, Xin Wang, and Carl Vondrick. 2022. Understanding zero-shot adversarial robustness for large-scale models. *arXiv preprint arXiv:2212.07016* (2022).
- [69] Xiangdi Meng, Damai Dai, Weiyao Luo, Zhe Yang, Shaoxiang Wu, Xiaochen Wang, Peiyi Wang, Qingxiu Dong, Liang Chen, and Zhifang Sui. 2024. PeriodicLoRA: Breaking the Low-Rank Bottleneck in LoRA Optimization. *arXiv preprint arXiv:2402.16141* (2024).
- [70] Jan Hendrik Metzen, Tim Genewein, Volker Fischer, and Bastian Bischoff. 2016. On Detecting Adversarial Perturbations. In *Proc. of ICLR*.
- [71] Tomas Mikolov, Ilya Sutskever, Kai Chen, Greg S Corrado, and Jeff Dean. 2013. Distributed representations of words and phrases and their compositionality. *Proc. of NeurIPS* (2013).
- [72] Erxue Min, Xifeng Guo, Qiang Liu, Gen Zhang, Jianjing Cui, and Jun Long. 2018. A survey of clustering with deep learning: From the perspective of network architecture. *IEEE Access* (2018).
- [73] John Morris, Eli Lifland, Jin Yong Yoo, Jake Grigsby, Di Jin, and Yanjun Qi. 2020. TextAttack: A Framework for Adversarial Attacks, Data Augmentation, and Adversarial Training in NLP. In *Proc. of EMNLP*.
- [74] Rui Pan, Xiang Liu, Shizhe Diao, Renjie Pi, Jipeng Zhang, Chi Han, and Tong Zhang. 2024. LISA: Layerwise Importance Sampling for Memory-Efficient Large Language Model Fine-Tuning. *arXiv preprint arXiv:2403.17919* (2024).
- [75] Tianyu Pang, Xiao Yang, Yinpeng Dong, Hang Su, and Jun Zhu. 2020. Bag of Tricks for Adversarial Training. In *Proc. of ICLR*.
- [76] Jing Pei, Lei Deng, Sen Song, Mingguo Zhao, Youhui Zhang, Shuang Wu, Guanrui Wang, Zhe Zou, Zhenzhi Wu, Wei He, et al. 2019. Towards artificial general intelligence with hybrid Tianjic chip architecture. *Nature* (2019).
- [120] Bryan A Plummer, Liwei Wang, Chris M Cervantes, Juan C Caicedo, Julia Hockenmaier, and Svetlana Lazebnik. 2015. Flickr30k entities: Collecting region-to-phrase correspondences for richer image-to-sentence models. In *Proc. of ICCV*.
- [78] Qi Qian. 2023. Stable Cluster Discrimination for Deep Clustering. In *Proc. of ICCV*.
- [79] Qi Qian, Yuanhong Xu, Juhua Hu, Hao Li, and Rong Jin. 2022. Unsupervised visual representation learning by online constrained k-means. In *Proc. of CVPR*.
- [80] Rushi Qiang, Ruiyi Zhang, and Pengtao Xie. 2024. BiLoRA: A Bi-level Optimization Framework for Overfitting-Resilient Low-Rank Adaptation of Large Pre-trained Models. *arXiv preprint arXiv:2403.13037* (2024).
- [81] Alec Radford, Jong Wook Kim, Chris Hallacy, Aditya Ramesh, Gabriel Goh, Sandhini Agarwal, Girish Sastry, Amanda Askell, Pamela Mishkin, Jack Clark, et al. 2021. Learning transferable visual models from natural language supervision. In *Proc. of ICML*.
- [82] Alec Radford, Karthik Narasimhan, Tim Salimans, Ilya Sutskever, et al. 2018. Improving language understanding by generative pre-training. (2018).
- [83] Aditya Ramesh, Prafulla Dhariwal, Alex Nichol, Casey Chu, and Mark Chen. 2022. Hierarchical text-conditional image generation with clip latents. *arXiv preprint arXiv:2204.06125* (2022).
- [84] Aditya Ramesh, Mikhail Pavlov, Gabriel Goh, Scott Gray, Chelsea Voss, Alec Radford, Mark Chen, and Ilya Sutskever. 2021. Zero-shot text-to-image generation. In *Proc. of ICML*.
- [85] Sylvestre-Alvise Rebuffi, Hakan Bilen, and Andrea Vedaldi. 2017. Learning multiple visual domains with residual adapters. *Proc. of NeurIPS* (2017).

- [86] Douglas A Reynolds. 2009. Gaussian mixture models. *Encyclopedia of biometrics* (2009).
- [87] Alex Rodriguez and Alessandro Laio. 2014. Clustering by fast search and find of density peaks. *science* (2014).
- [88] Robin Rombach, Andreas Blattmann, Dominik Lorenz, Patrick Esser, and Björn Ommer. 2022. High-resolution image synthesis with latent diffusion models. In *Proc. of CVPR*.
- [89] Meitar Ronen, Shahaf E Finder, and Oren Freifeld. 2022. Deepdpm: Deep clustering with an unknown number of clusters. In *Proc. of CVPR*.
- [90] Muhammad Yahya Saeed, Muhammad Awais, Ramzan Talib, and Muhammad Younas. 2020. Unstructured text documents summarization with multi-stage clustering. *IEEE Access* (2020).
- [91] Mahmood Sharif, Sruti Bhagavatula, Lujo Bauer, and Michael K Reiter. 2016. Accessorize to a crime: Real and stealthy attacks on state-of-the-art face recognition. In *Proceedings of the 2016 acm sigsac conference on computer and communications security*. 1528–1540.
- [92] Christian Szegedy, Wojciech Zaremba, Ilya Sutskever, Joan Bruna, Dumitru Erhan, Ian Goodfellow, and Rob Fergus. 2013. Intriguing properties of neural networks. *arXiv preprint arXiv:1312.6199* (2013).
- [93] Ashish Vaswani, Noam Shazeer, Niki Parmar, Jakob Uszkoreit, Llion Jones, Aidan N Gomez, Łukasz Kaiser, and Illia Polosukhin. 2017. Attention is all you need. *Proc. of NeurIPS* (2017).
- [94] Rajagopal Venkatesaramani, Bradley A Malin, and Yevgeniy Vorobeychik. 2021. Re-identification of individuals in genomic datasets using public face images. *Science advances* (2021).
- [95] Riccardo Volpi, Hongsok Namkoong, Ozan Sener, John C Duchi, Vittorio Murino, and Silvio Savarese. 2018. Generalizing to unseen domains via adversarial data augmentation. *Proc. of NeurIPS* (2018).
- [96] Ulrike Von Luxburg. 2007. A tutorial on spectral clustering. *Statistics and computing* (2007).
- [121] Haixin Wang, Xinlong Yang, Jianlong Chang, Dian Jin, Jinan Sun, Shikun Zhang, Xiao Luo, and Qi Tian. 2023. Parameter-efficient Tuning of Large-scale Multimodal Foundation Model. In *Proc. of NeurIPS*.
- [98] Sheng Wang, Liheng Chen, Jiyue Jiang, Boyang Xue, Lingpeng Kong, and Chuan Wu. 2024. LoRA Meets Dropout under a Unified Framework. *arXiv preprint arXiv:2403.00812* (2024).
- [99] Yu-Xiong Wang, Deva Ramanan, and Martial Hebert. 2017. Growing a brain: Fine-tuning by increasing model capacity. In *Proc. of CVPR*.
- [100] Zirui Wang, Jiahui Yu, Adams Wei Yu, Zihang Dai, Yulia Tsvetkov, and Yuan Cao. 2021. Simvlm: Simple visual language model pretraining with weak supervision. *arXiv preprint arXiv:2108.10904* (2021).
- [101] Xingxing Wei, Jun Zhu, Sha Yuan, and Hang Su. 2019. Sparse adversarial perturbations for videos. In *Proc. of AAAI*.
- [102] Mitchell Wortsman, Gabriel Ilharco, Jong Wook Kim, Mike Li, Simon Kornblith, Rebecca Roelofs, Raphael Gontijo Lopes, Hannaneh Hajishirzi, Ali Farhadi, Hongsok Namkoong, et al. 2022. Robust fine-tuning of zero-shot models. In *Proc. of CVPR*.
- [103] Wenhao Wu, Zhun Sun, and Wanli Ouyang. 2022. Transferring textual knowledge for visual recognition. *arXiv preprint arXiv:2207.01297* (2022).
- [104] Junyuan Xie, Ross Girshick, and Ali Farhadi. 2016. Unsupervised deep embedding for clustering analysis. In *Proc. of ICML*.
- [105] Yinghui Xing, Qirui Wu, De Cheng, Shizhou Zhang, Guoqiang Liang, and Yanning Zhang. 2022. Class-aware visual prompt tuning for vision-language pre-trained model. *arXiv preprint arXiv:2208.08340* (2022).
- [122] Jun Xu, Tao Mei, Ting Yao, and Yong Rui. 2016. Msr-vtt: A large video description dataset for bridging video and language. In *Proc. of CVPR*.
- [107] Jianwei Yang, Devi Parikh, and Dhruv Batra. 2016. Joint unsupervised learning of deep representations and image clusters. In *Proc. of CVPR*.
- [108] Zhixiong Zeng and Wenji Mao. 2022. A comprehensive empirical study of vision-language pre-trained model for supervised cross-modal retrieval. *arXiv preprint arXiv:2201.02772* (2022).
- [109] Haotian Zhang, Pengchuan Zhang, Xiaowei Hu, Yen-Chun Chen, Liunan Li, Xiyang Dai, Lijuan Wang, Lu Yuan, Jenq-Neng Hwang, and Jianfeng Gao. 2022. Glipv2: Unifying localization and vision-language understanding. *Proc. of NeurIPS* (2022).
- [110] Qingru Zhang, Minshuo Chen, Alexander Bukharin, Pengcheng He, Yu Cheng, Weizhu Chen, and Tuo Zhao. 2023. Adaptive budget allocation for parameter-efficient fine-tuning. *arXiv preprint arXiv:2303.10512* (2023).
- [111] Qingzhao Zhang, Shengtuo Hu, Jiachen Sun, Qi Alfred Chen, and Z Morley Mao. 2022. On adversarial robustness of trajectory prediction for autonomous vehicles. In *Proc. of CVPR*.
- [112] Jiawei Zhao, Zhenyu Zhang, Beidi Chen, Zhangyang Wang, Anima Anandkumar, and Yuandong Tian. 2024. Galore: Memory-efficient llm training by gradient low-rank projection. *arXiv preprint arXiv:2403.03507* (2024).
- [113] Yunqing Zhao, Tianyu Pang, Chao Du, Xiao Yang, Chongxuan Li, Ngai-Man Cheung, and Min Lin. 2023. On evaluating adversarial robustness of large vision-language models. *arXiv preprint arXiv:2305.16934* (2023).
- [114] Ming Zhong, Yelong Shen, Shuohang Wang, Yadong Lu, Yizhu Jiao, Siru Ouyang, Donghan Yu, Jiawei Han, and Weizhu Chen. 2024. Multi-LoRA Composition for Image Generation. *arXiv preprint arXiv:2402.16843* (2024).
- [115] Kaiyang Zhou, Jingkang Yang, Chen Change Loy, and Ziwei Liu. 2022. Learning to prompt for vision-language models. *International Journal of Computer Vision* (2022).
- [116] Lisa Anne Hendricks, Oliver Wang, Eli Shechtman, Josef Sivic, Trevor Darrell, and Bryan Russell. 2017. Localizing moments in video with natural language. In *Proc. of ICCV*.
- [117] Max Bain, Arsha Nagrani, Gül Varol, and Andrew Senior. 2021. Frozen in time: A joint video and image encoder for end-to-end retrieval. In *Proc. of ICCV*. 1728–1738.
- [118] Tsung-Yi Lin, Michael Maire, Serge Belongie, James Hays, Pietro Perona, Deva Ramanan, Piotr Dollár, and C Lawrence Zitnick. 2014. Microsoft coco: Common objects in context. In *Proc. of ECCV*.
- [119] Haoyu Lu, Mingyu Ding, Yuqi Huo, Guoxing Yang, Zhiwu Lu, Masayoshi Tomizuka, and Wei Zhan. 2023. UniAdapter: Unified Parameter-Efficient Transfer Learning for Cross-modal Modeling. *arXiv preprint arXiv:2302.06605* (2023).
- [120] Bryan A Plummer, Liwei Wang, Chris M Cervantes, Juan C Caicedo, Julia Hockenmaier, and Svetlana Lazebnik. 2015. Flickr30k entities: Collecting region-to-phrase correspondences for richer image-to-sentence models. In *Proc. of ICCV*.
- [121] Haixin Wang, Xinlong Yang, Jianlong Chang, Dian Jin, Jinan Sun, Shikun Zhang, Xiao Luo, and Qi Tian. 2023. Parameter-efficient Tuning of Large-scale Multimodal Foundation Model. In *Proc. of NeurIPS*.
- [122] Jun Xu, Tao Mei, Ting Yao, and Yong Rui. 2016. Msr-vtt: A large video description dataset for bridging video and language. In *Proc. of CVPR*.